Proc. Indian natn. Sci. Acad., **60**, A, No. 1, 1994, pp. 171-179.

THE NOR'WESTER SCENARIO: THE ROLE OF INTERNAL GRAVITY WAVE

D K SINHA AND G K SEN
Centre for Atmospheric Sciences, University of Calcutta,
92, *Acharya Prafulla Chandra Road, Calcutta* 700 019, *India*

(*Received* 15 *June* 1993; *Accepted* 17 *June* 1993)

The understanding of the development of Nor'westers, through the mechanism of momentum and energy transfer of Internal Gravity Wave, forms the chief interest of this paper. A simulation experiment has been done to show that due to such transfer processes with changing phase velocity of disturbances, lower stable layer turns out to be unstable with significant growth as phase velocity approaches the true storm speed of that day. The findings also reveal the role of upper and lower layers in storm-triggering processes.

Key Words: Nor'Westers Scenario; Internal Gravity Wave; Momentum; Energy Transfer; Storm-triggering

Introduction

Nor'westers are known to be severe storms that are dominantly characteristic of the eastern part of India occurring usually between March and preonset phase of the Indian summer monsoon. These storms usually come from Northwest, being developed deeply in Chotanagpur belt, *vide*, *Tech. Rep.* IMD No. 10 (1941)[1]. This storm travels along Northwest to Southeast direction with a speed of 30 to 40mph and is normally accompanied by strong surface winds, hailstorms and often tornadoes. The extant literature on such storms says that a very tall cloud growth is an associated feature; it is a mesoscale process where horizontal scale is comparable to vertical scale; in fact, according to Rao and Mukherjee[2], there can be cloud development upto an altitude of 20km. This storm can last from 30 min. to several hours; Koteswaram and Chakraborty[3] pointed out the importance of Chotanagpur belt of Bihar plateau in initiating vigorous convection, which is apparent from the development of convective clouds over the slopes of high terrain, Ramaswamy[4], through his extensive analysis of sea level and upper air chart, pointed out that the dynamics of middle and upper tropospheric west wind belt and thermal advection process are more potent to Nor'westers. He also found wave pattern in jet stream which is a conspicuous feature of 700-500mb and 500-300mb partial thickness line. Koteswaram and Srinivasan[5] mentioned that development of Nor'westers associated thunderstorm is possible due to superposition of upper divergence associated with a straight jet, anticyclonic vortex on convergence associated with low level flow, even southernly flow. As most of the thunderstorms start in the afternoon, the role of insolation and orography in triggering thunderstorms is also an additional feature. These investigations lead us to the fact that Nor'westers, having originated in areas close to Chotanagpur belt of Bihar, chiefly occur on account of the strong influence of convection; and its dynamics is controlled by strong wind shear at lower and upper troposphere, with a strong moisture content at lower levels. The time of occurrence of such storms, their speed and its horizontal length scale, continue to be basic concerns for in-depth studies of Nor'wester phenomena, particularly the understanding of physical processes involved.

In atmospheric phenomena concerning storms, it is customary to seek understanding of the physics of the development of storms from different standpoints. One kind of investigation in respect of storm generation is to study, how an Internal Gravity Wave (IGW) influences the transport of energy and momentum from higher to lower levels leading to an augmentation of wind speed, thereby increasing instability at lower levels, *vide* Gossard and Hook[6], King *et al.*[7], Lalas and Einaudi[8], Lin and Goff[9], Lindzen[10], Gill[11] and Gossard and Moninger[12]. To the best of knowledge of the authors, the study of development of Nor'westers has not been looked into so far from this standpoint. The purpose of the present paper is to establish, from theoretical standpoint reinforced by available data, the existence of Internal Gravity Wave (IGW) thereby facilitating understanding of possible mechanisms for transport of momentum and energy to the lower levels. The layout of this paper is as follows.

To begin with, a description of the model of internal gravity wave drawing upon the works of Lindzen[10] and Gill[11], is set forth. Then comes the method of solution followed by an analysis, from theoretical considerations, of the estimation of parameters. Next to provide a realistic flavour of this investigation on propagation of internal gravity wave affecting stability or otherwise in subsequent stages, we perform a simulation experiment on the basis of IMD data.

A critical analysis of profiles obtained from the experiment provides us a better insight about the processes of energy and momentum transfers through IGW leading to conspicuous instability at lower levels.

Model Description

For a basic flow with vertical shear $\left(\frac{\partial u}{\partial z}, \frac{\partial v}{\partial z}\right)$ in the z-direction, the equations of

motion, continuity and energy conservation are, *vide*, Lindzen[10], Gill[11].

$$\rho\left\{\frac{\partial}{\partial t}+u\frac{\partial}{\partial x}+v\frac{\partial}{\partial y}+w\frac{\partial}{\partial z}\right\}u=-\frac{\partial p}{\partial x}, \qquad \ldots (1)$$

$$\rho\left\{\frac{\partial}{\partial t}+u\frac{\partial}{\partial x}+v\frac{\partial}{\partial y}+w\frac{\partial}{\partial z}\right\}v=-\frac{\partial p}{\partial y}, \qquad \ldots (2)$$

$$\rho\left\{\frac{\partial}{\partial t}+u\frac{\partial}{\partial x}+v\frac{\partial}{\partial y}+w\frac{\partial}{\partial z}\right\}w=-\frac{\partial p}{\partial z}-g\rho \qquad \ldots (3)$$

and

$$\left\{\frac{\partial}{\partial t}+u\frac{\partial}{\partial x}+v\frac{\partial}{\partial y}+w\frac{\partial}{\partial z}\right\}\rho+\rho\left(\frac{\partial u}{\partial x}+\frac{\partial v}{\partial y}+\frac{\partial w}{\partial z}\right)=0\,. \qquad \ldots (4)$$

Taking the atmosphere to be a Boussinesq fluid, we can split eq. (4) into two equations:

$$\left\{\frac{\partial}{\partial t}+u\frac{\partial}{\partial x}+v\frac{\partial}{\partial y}+w\frac{\partial}{\partial z}\right\}\rho=0\,. \qquad \ldots (5)$$

(under the incompressibility condition)

$$\frac{\partial u}{\partial x}+\frac{\partial v}{\partial y}+\frac{\partial w}{\partial z}=0 \qquad \ldots (6)$$

Here u, v, w, ρ, p are zonal velocity, meridional velocity, vertical velocity, density and pressure respectively. The independent variables are time (t), zonal direction (x), meridional direction (y) and vertical direction z. As usual, we now expand the state variables into basic and perturbed parts.

$$\begin{aligned}
u &= u_0(z)+u'(x,y,z,t)\,,\\
v &= v_0(z)+v'(x,y,z,t)\,,\\
w &= w'(x,y,z,t)\,, \qquad \ldots (7)\\
\rho &= \rho_0(z)+\rho'(x,y,z,t)
\end{aligned}$$

and

$$p=p_0(z)+p'(x,y,z,t)\,.$$

It is to be remarked, in passing, that both meridional and zonal velocities are important for Nor'wester development. Here, we have retained both the unperturbed velocities for u and v, disturbances being from North-Western side to travel along South-Eastern direction. We next construct the linearized equation and then adopt the following transformation of perturbed variables as

$$\left[u',\,v',\,w',\,\frac{1}{p'}\right]=\left(\frac{\rho_s}{\rho_0}\right)^{1/2}\left[U,\,V,\,W,\,\frac{1}{p}\right] \qquad \ldots (8)$$

The unperturbed vertical velocity, being negligible, is omitted. This is also warranted by our subsequent simulation experiment which presupposes a stable state of thermal stratification.

Here $\rho_0(z)$ is the unperturbed density and ρ_s is the density at surface.

The resulting partial differential equation, is linear in U, V, W and P'; we seek its solution being in the form:

$$\begin{aligned}
U &= U(z)\sin(kx+ly-\sigma t);\\
V &= V(z)\sin(kx+ly-\sigma t); \qquad \ldots (9)\\
W &= W(z)\cos(kx+ly-\sigma t);\ \text{and}\\
P &= P(z)\sin(kx+ly-\sigma t).
\end{aligned}$$

Elimination of $U(z)$, $V(z)$ and $P(z)$ leads to the ordinary differential equation in $W(z)$:

$$\frac{d^2 W}{dz^2} + \alpha(z)\, W(z) = 0\,, \qquad \ldots (10)$$

where

$$\alpha(z) = -m^2 + \frac{1}{\omega}\left[k\frac{d^2 u_0}{dz^2} + l\frac{d^2 v_0}{dz^2}\right] + \left(\frac{Nm}{\omega}\right)^2,$$

$$\omega = k\left(C - u_0 - \frac{l}{k}\, v_0\right)$$

and

$$m^2 = l^2 + k^2,\ C = \frac{\sigma'}{k},\ N^2 = -\frac{g}{\rho_s}\frac{d\rho}{dz} = \frac{g}{\theta_v}\frac{d\theta_v}{dz} \qquad \ldots (11)$$

Here l and k are horizontal wave numbers along zonal and meridional direction, σ is the wave angular frequency. C is the phase speed. N^2 is the Brunt-Vaisala frequency, θ_v is the virtual potential temperature, ω is the expression for intrinsic frequency.

The solution of eq. (10) is sought for a multilayered model. At the surface, assumed to be a rigid level, we set $W=0$. At the interface between several layers, the kinematic condition is $W_L = W_U$ and dynamic condition is $P_L = P_U$, *where* L represents lower and U upper layer, *vide*, Gossard and Hook[6]. It is to be noted that both w and dw/dz are continuous at the interface. This is also true for the undisturbed interface.

Method of Solution

We first compute $\alpha(z)$ at several grid points along vertical, where measured values of atmospheric variables are available from Radiosonde data, *vide* IMD[1]. After computing the values of $\alpha(z)$ we divide the atmosphere into several layers where in each layer $\alpha(z)$ profile is either concave or convex. From each layer, we choose three grid points one at the bottom of layer, one at the top of layer and another, in between where $\alpha(z)$ attains either minimum or maximum value i.e., $\frac{d\alpha}{dz} = 0$. Using the three values of $\alpha(z)$ at these three points, we try to fit them using a function of the form

$$\alpha(z) = -\frac{\mu^2}{4} + \frac{E^2}{(1 + D_1 e^{\mu z} + D_2 e^{-\mu z})^2} \qquad \ldots (12)$$

So in each layer, we have an estimate of μ, E, D_1 & D_2 respectively. Then we also estimate K_r and K_i to be used later on, from the relation

$$K^2 = E^2 + \mu^2(D_1 D_2 - 1), \qquad \ldots (13)$$

where $K_r = \sqrt{K^2}$ if $K^2 > 0$ and $K_i = \sqrt{-K^2}$ if $K^2 < 0$.

For $K^2 > 0$ i.e., $K_r \neq 0$ and $K_i = 0$ the final solution is of the form

$$W = \sqrt{|1 + D_1 e^{\mu z} + D_2 e^{-\mu z}|}\,(C_1 \sin\theta + C_2 \cos\theta), \qquad \ldots (14)$$

where

$$\theta = \frac{\cdot\, 2(K_r + K_i)}{\mu\sqrt{4D_1D_2 - 1}} \left\{ \tan^{-1}\left(\frac{1 + 2D_1 e^{\mu z}}{\sqrt{4D_1D_2 - 1}}\right) - \tan^{-1}\left(\frac{1 + 2D_1 e^{\mu z_0}}{\sqrt{4D_1D_2 - 1}}\right) \right\}, \qquad \ldots (15)$$

when

$4D_1D_2 - 1 > 0$

and

$$\theta = \frac{(K_r + K_i)}{\mu\sqrt{4D_1D_2 - 1}} \left\{ \log_e \frac{(1 + 2D_1 e^{\mu z}) - \sqrt{1 - 4D_1D_2}}{(1 + 2D_1 e^{\mu z}) + \sqrt{1 - 4D_1D_2}} - \log_e \frac{(1 + 2D_1 e^{\mu z_0}) - \sqrt{1 - 4D_1D_2}}{(1 + 2D_1 e^{\mu z_0}) + \sqrt{1 - 4D_1D_2}} \right\} \qquad \ldots (16)$$

when

$4D_1D_2 - 1 < 0$

for $K^2 < 0$ i.e., $K_r = 0$ and $K_i = 0$,

$$W(z) = \sqrt{|1 + D_1 e^{\mu z} + D_2 e^{-\mu z}|}\,[C_1 \sinh\theta + C_2 \cosh\theta]. \qquad \ldots (17)$$

The expressions of θ, are same, as described by (16) and (15) Z_0 is the height of lower boundary of each layer.

Our next task is to match the values of $w(z)$ and $\frac{dw}{dz}$ at the interface of each layer. It is also important to satisfy the lower boundary condition. This enables us to estimate the values of constants c_1 and c_2 in each layer.

Simulation Experiment: Analysis and Discussion

As stated earlier, this experiment is based on IMD data set. The period of observation is from May 10, 1988 to May 25, 1988. The data consisting of usual radiosonde observations. are taken 4 times daily at 5-30 IST, 10-45 IST, 17-30 IST and 22-45 IST at five stations Calcutta, Bhubaneswar, Ranchi, Patna and Siliguri. On 22-05-1988 at Calcutta a Nor'wester storm occurred at 19-40 IST. The characteristic horizontal length scale of this disturbance is 20km. The data we have used here is the radiosonde observation taken at 0 GMT or 5-30 IST at Calcutta on 22-05-1988, which is 14 hours prior to storm. Let us now have an indepth analysis on the stability or otherwise of the internal gravity wave on the basis of modelling, done earlier and simulation. This allows the phase ve-

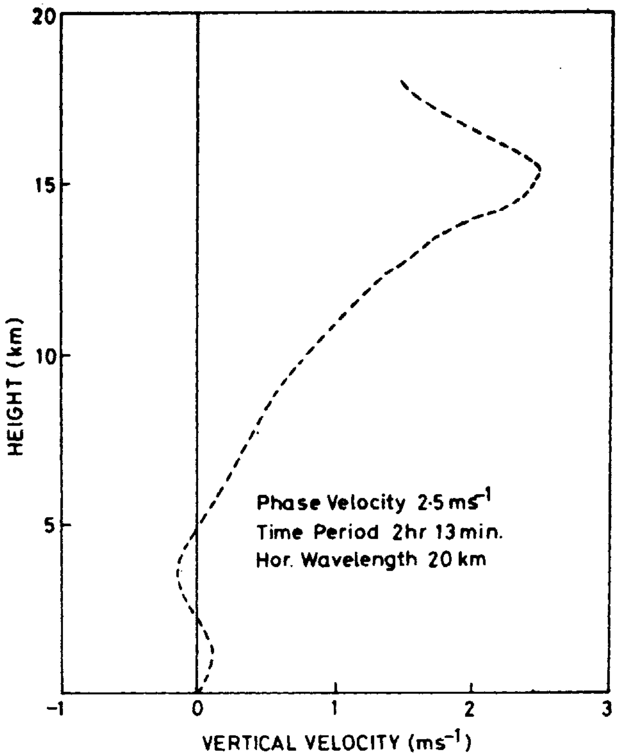

Fig 1

locity to assume appropriate values sequentially close to the known value of the storm speed, as available from IMD data. What we seek precisely here is to get at positive or negative values of K^2, given by eq. (13), enabling us to have a qualitative information about stability or instability of the layer concerned. In mathematical terms, this is an eigenvalue problem. Accordingly, the simulation experiment is structured as follows:

In order to analyse our findings, we draw the profiles of perturbed vertical velocity versus height. Fig. 1, provides the graph of the first experiment with phase velocity 2.5 ms^{-1}; one also finds internal gravity waves with wave length 4.5km, obviously well below 5km indicative of its existence in lower tropospheric levels. The 5-15km level, shows a growth of amplitude with its maximum at 15km. It is found that K^2 is negative throughout this layer. Hence, any perturbation at 15km. level will have the maximum amplitude and propagate downward as internal gravity wave. This is generated because of a horizontally propagating disturbance with length scale 20km and speed 2.5ms^{-1}.

The second step in the experiment is to increase the phase velocity to 5.55ms^{-1} and the profiles are drawn in Fig. 2. The internal gravity wave in this case is of a very small amplitude and vertical wavelength 4km. A growth on account of instability is observed in the layer 4-13km. Then follows a remarkable growth (through negative amplitude increment) with a maximum at 16.5km. In passing, one finds strikingly a negative amplitude, contrary to posi-

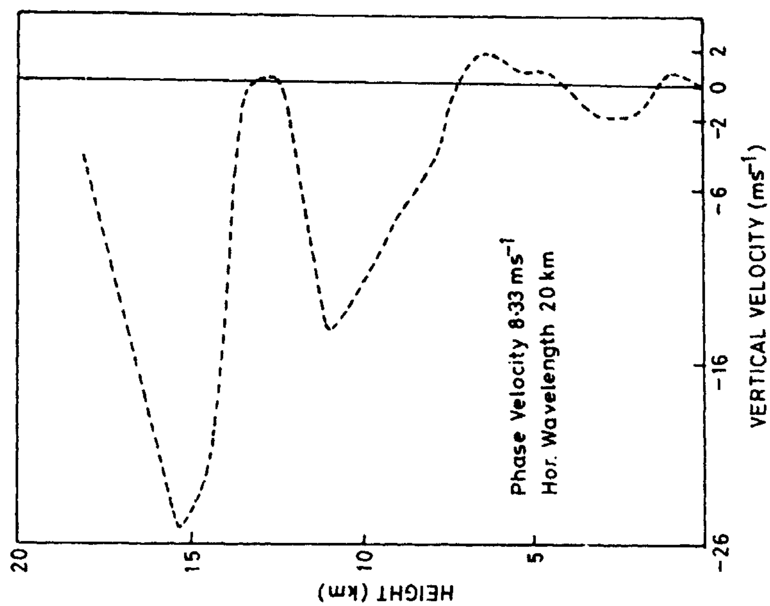
Phase Velocity 8·33 ms^{-1}
Hor. Wavelength 20 km
HEIGHT (km)
VERTICAL VELOCITY (ms^{-1})
20
15
10
5
−26
−16
−6
−2
0
2

Fig 3

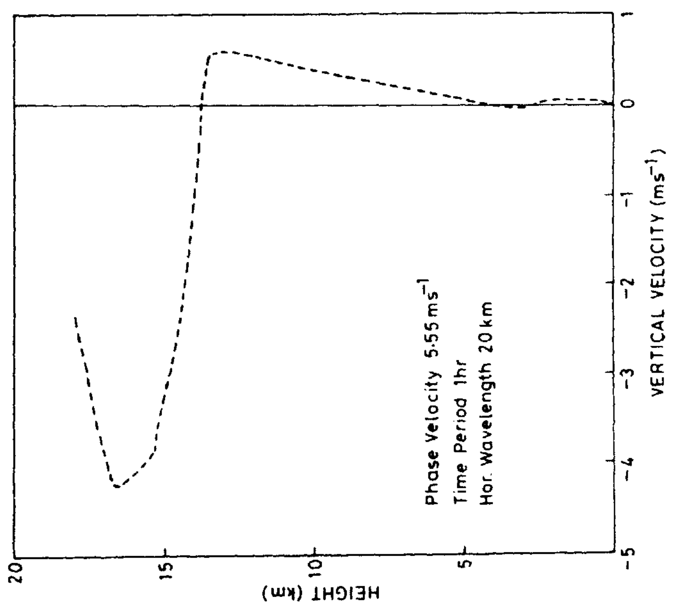
Phase Velocity 5·55 ms^{-1}
Time Period 1hr
Hor. Wavelength 20 km
HEIGHT (km)
VERTICAL VELOCITY (ms^{-1})
20
15
10
5
−5
−4
−3
−2
−1
0
1

Fig 2

tive amplitude in the earlier experiment above 13km level. Further, the updraft zone has decreased in height with the increase of phase speed, and one can thus call it a strong downdraft zone, roughly above 14km, which was not observed in the first experiment.

The phase velocity of the third experiment (Fig. 3) is 8.33ms^{-1} or 30km. per hour. Here $K^2 < 0$, for $Z < 2$km, $7 < Z < 12$km, $13 < Z < 15$km. The internal gravity wave generated at 15km. level, as before, propagates downward. The modes at several other layers being unstable, it is likely that the internal gravity wave generated at 11km level may also propagate downward. It thus looks possible that the internal gravity wave generated in the level $13 < Z < 15$km in its downward propagation, has its amplitude augmented in the unstable layer between 7 and 12km, strictly at 11km level, even though it may suffer otherwise. The vertical wavelength is 4km. The downdraft zone is clearly within $7 < Z < 12$km. One may think in terms of possibility of cloud in this layer of 5km thick.

In the final experiment, the phase velocity is 8.9ms$^{-1}\cdot$32km hr^{-1}. The outcome is shown in Fig. 4. A strong downward draft from 1km to 2.3km is observed. Further, below, 1km. a weak updraft is observed, which characterises a feature of weak convection before storm, as as is obvious from 1730 sounding.

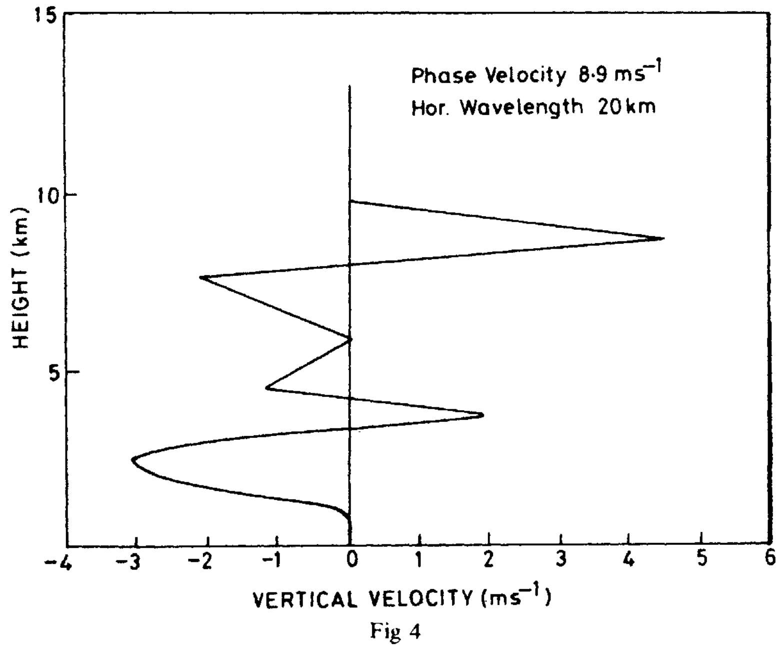

Fig 4

A comparative study of all the four experiments may now be undertaken First, from Figs 1 and 2, we find that, for a low phase speed of propagation, the Internal Gravity Wave with vertical wavelength 4 to 4.5km is observed. In such a case, phase speed is below 5.5ms^{-1}. Second, in all the cases, Internal Gravity Wave is generated at 15km level, due to the existence of instability. Third, while the increase in phase speed makes all gravity wave modes more and more unstable, the increase in amplitude takes place at lower levels. Specifically speaking, with increased value of the phase speed and constant horizontal wavelength, the lower troposphere is found to exhibit more instability than what it was at low phase speed. Hence, it is surmised that at higher phase speed of disturbance, the momentum and energy transport by Internal Gravity Wave, which is, of course, generated at higher unstable layer, are increased. Finally the lower troposphere becoming unstable as disturbance attains phase speed of 32km hr^{-1}, one observes a beginning of strong downdraft which becomes often obvious before storms.

Conclusions

The foregoing investigation, even though essentially theoretical in nature, brings out an interesting feature of generating IGW between 4-13km layer because of instability. While this is not somewhat unusual in respect of IGW in the context of severe thunderstorm as observed through satellite observation on cloud elsewhere *vide* Ley and Peltier[13], findings here in respect of Nor'westers show a striking resemblance to the observational findings on the existence of simply waves in that form as observed by Ramaswamy[4]. Further, that instability can occur in a few specific layers, namely 4-11km layers is also revealed from this investigation, and this finds a fairly close agreement with what have been indicated by Koteswaram and Srinivasan[5].

Acknowledgement

Authors wish to thank the Department of Science & Technology, Government of India for financial support and IMD for data provided to them.

References

1 India Meteorological Department (IMD) (1941) *Nor'westers of Bengal Tech Note* No. 10
2 D V Rao and A K Mukherjee *Indian J Met Geophys* **1** (1958) 313-322
3 P Koteswaram and K C Chakraborty *Indian J Met Geophys* **1** (1950) P-167
4 C Ramaswamy *Tellus* **8** (1956)
5 P Koteswaram and V Srinivasan *Indian J Met Geophys* **9** (1958) 301.
6 E E Gossard and W H Hook *Waves in the Atmosphere* Elsevier Scientific Publication, New York (1975) 456
7 J C King, S D Mobbs, M S Derby and J M Rees *Bound Layer Met* **39** (1987) 1-13
8 D P Lalas and F Eïssandi *J appl Met* **13** (1974) 318-324
9 Y H Lin and R C Goff *J atmos Sci* **45** (1988) 194-205
10 R S Lindzen *Dynamics in Atmospheric Physics* Cambridge University Press, Cambridge (1990)
11 F A Gill *Atmosphere Ocean Dynamics* Academic Press, New York (1982)
12 E E Gossard and W R Moninger *J atmos Sci* **32** 2111-2123
13 E B Ley and W R Peltier *J atmos Sci* **38** (1981) p1206